Molecular Crystals and Liquid Crystals
Publication details, including instructions for authors and subscription information:
http://www.tandfonline.com/loi/gmcl16

Naphthalene-Rare Gas Solids: Absorption Spectra from 30000-30000 cm^{-1}

J. G. Angus [a] [b] & G. C. Morris [a]
[a] Department of Chemistry, University of Queensland, St. Lucia, 4067, Australia
[b] Department of geology, The University, Manchester, M139PL, England
Version of record first published: 28 Mar 2007.

To cite this article: J. G. Angus & G. C. Morris (1970): Naphthalene-Rare Gas Solids: Absorption Spectra from 30000-30000 cm^{-1}, Molecular Crystals and Liquid Crystals, 11:3, 257-277

To link to this article: http://dx.doi.org/10.1080/15421407008083518

Molecular Crystals and Liquid Crystals. 1970. Vol. 11, pp. 257–277

Printed in Great Britain

Naphthalene–Rare Gas Solids: Absorption Spectra from 30000–80000 cm^{-1}

J. G. ANGUS† and G. C. MORRIS

Department of Chemistry
University of Queensland
St. Lucia 4067
Australia

Received August 17, 1970

Abstract—The absorption spectra (30000–80000 cm^{-1}) of naphthalene–rare gas solids (molar ratio 1:200) are reported. The congested band system in the region of the second $\pi^*-\pi$ transition is analysed. Observed higher $\pi^*-\pi$ transitions are compared with theoretical predictions. The assignments of the lowest ($n = 3$) Rydberg states (with different quantum defects) to bands observed in the free molecule spectrum at 45070 cm^{-1} and 45390 cm^{-1} is supported. Intermediate and large radius impurity states of the matrix are identified and characterized. Crystal energy parameters for the matrix are deduced from spectroscopic data and photoemission data. Matrix shifts for the origin bands of the first four $\pi^*-\pi$ transitions are reported.

1. Introduction

Experimental studies of the two lowest $\pi^*-\pi$ singlet transitions of naphthalene (vapor,[1,2,3] solution,[4,5] solid solution[6,7,8] and crystal[9,10,11,12] have tested the adequacy of quantum mechanical descriptions of the π electron systems of aromatic molecules[13,14] and increased the understanding of electronic states in aromatic solids.[15,16,17] The results show the electronic assignments of the first and second singlet transitions to be $B_{2u} \leftarrow A_{1g}$ (long axis polarized) and $B_{1u} \leftarrow A_{1g}$ (short axis polarized) respectively. The total oscillator strength of the first transition is enhanced by "intensity borrowing" from the second transition.[18] The third and fourth (singlet) transitions are predicted[19,20,21] near 50000 cm^{-1} with electronic assignments $B_{2u} \leftarrow A_{1g}$ and $B_{1u} \leftarrow A_{1g}$ respectively.

† Present address: Department of Geology, The University, Manchester, M139PL, England.

Skanke[22] has assigned the fourth transition to a broad absorption band in the solution spectrum[23] between 58000 and 61000 cm^{-1} but George and Morris[24] place this transition at 49500 cm^{-1} in the vapor. Although there has been little reported for the spectral region above 40000 cm^{-1}, some firm results are known. The major features in the free molecule absorption spectrum from 40000 to 75000 cm^{-1} are an extensive Rydberg system overlying inhomogeneously broadened absorption bands[25,26] with effects arising from interference between resonance and potential scattering.[27]

The spectrum of the molecule trapped in low temperature–rare gas matrices yields more detailed information about certain excited electronic states than is available from the vapor or solution spectrum for several reasons: (a) spectral congestion arising from hot bands and sequence structure is removed; (b) matrix shifts help to distinguish vibronic bands of different electronic origins; (c) the variation of the transition energies of the molecule in different matrices helps to distinguish intravalence (π^*–π) and extravalence (Rydberg) transitions. Further such studies help to understand how best to describe the energy states of impurity doped solids.

We have investigated the absorption spectrum, between 30000 and 80000 cm^{-1}, of naphthalene (*h*–8 and *d*–8) trapped in argon, krypton and xenon matrices. From this work we (a) analyse the congested band system in the region of the second π^*–π transition; (b) confirm the assignment of the fourth π^*–π transition suggested by George and Morris[24]; (c) support an assignment[26] of the lowest ($n = 3$) Rydberg states of the molecule; (d) analyse the structure of the π^*–π transitions which are obscured in the free molecule spectrum by the intense Rydberg system; (e) identify and characterize intermediate and large radius impurity states of the matrix.

2. Experimental

Naphthalene was purified by sodium fusion and extensive zone refining.[24] Spectrographically pure xenon, krypton and argon gases (from British Oxygen Co.) were further purified over a freshly sputtered titanium film. Matrices were prepared by codeposition from the vapor onto a lithium fluoride disc maintained at *ca.* 40 °K. The thickness of the films varied between *ca.* 0.5 and 5 μ and the

naphthalene–rare gas molar ratio was in the order of 1 : 200. After a period of thermal annealing (*ca.* 30 min) the films were cooled to 20 °K. This procedure minimized the site splitting effects in the spectrum and produced films which did not scatter the incident radiation excessively. The sample holder was maintained at selected temperatures between 20 °K and 50 °K by use of an open cycle Joule Thomson refrigerator with hydrogen gas and liquid nitrogen as refrigerants. Spectra were recorded photoelectrically on a 0.5 m Jarrell Ash vacuum ultraviolet spectrometer using equivalent slit widths of 0.5 Å. Light source continua were a hydrogen arc (to 51 KK) and microwave powered xenon and krypton lamps (to 80 KK). Emission lines in the source were used for calibration. The sample holder was located between the exit slit of the spectrometer and the photomultiplier to minimize photodecomposition. Because of the difficulty in correcting for scatter of the incident radiation and luminescence excitation in this experimental design only relative absorption intensities are quoted. Matrix induced line broadening is significant for a large guest molecule such as naphthalene and the accuracy of the measured transition energies varies from ± 20 cm^{-1} to ± 100 cm^{-1} depending on the line width of the absorption band.

3. Results and Discussion

3.1. Spectral Region 320 nm–250 nm

The absorption spectra between 250 nm and 320 nm of naphthalene–argon, naphthalene–krypton and naphthalene–xenon matrices (molar ratio 1 : 200) are shown in Fig. 1. The region between 272 and 290 nm in the spectra of krypton and xenon matrices is expanded to illustrate some features more clearly. Transition energies and suggested assignments are given in Table 1. In Table 2 the vibrational intervals measured in this work are compared with corresponding values from the vapor spectrum.[1] Included in this table are the ground state fundamentals identified in the Raman spectrum of the single crystals.[28]

Polarized absorption and fluorescence spectra of naphthalene in low temperature solid solutions[6,7] have shown the first and second π^*–π transitions to be long axis ($B_{2u} \leftarrow A_{1g}$) and short axis ($B_{1u} \leftarrow A_{1g}$)

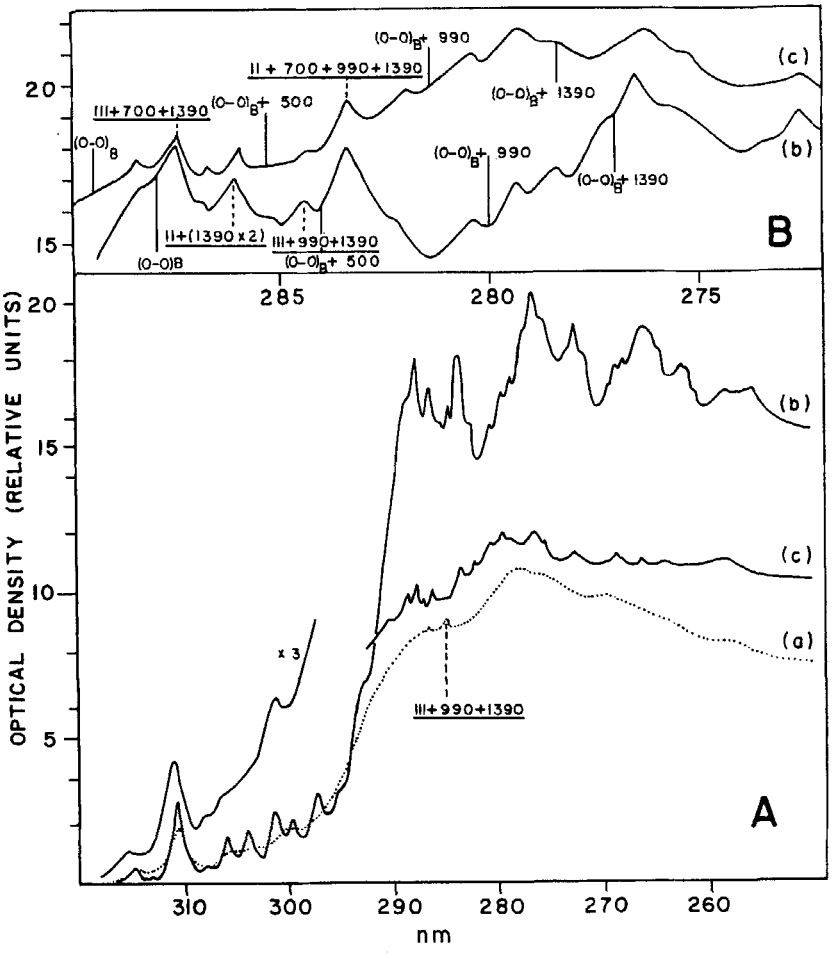

Figure 1. (A) The absorption spectra from 320 nm to 250 nm of naphthalene doped argon (Curve *a*), krypton (Curve *b*) and xenon (Curve *c*) solids at 20 °K. Deposition temperature 40 ± 2 °K, molar ratios (naphthalene–rare gas) 1 : 200. (B) The absorption spectra (272 nm to 290 nm) of naphthalene doped krypton (Curve *a*) and xenon (Curve *b*) solids at 20 °K.

polarized respectively. The vibronic structure of the first transition may be divided into three major series.

Series I: A series of low intensity corresponding to progressions of totally symmetric (a_{1g}) vibrations built upon the electronic origin ($B_{2u} \leftarrow A_{1g}$).

TABLE 1 Transition Energies (cm^{-1}) and Suggested Assignments in the Absorption Spectra of Naphthalene Doped Argon, Krypton and Xenon Solids

Argon	Krypton	Xenon	Suggested assignments
31800±50	31770±30	31750±40	$(O—O)_A(B_{2u} \leftarrow A_{1g})$: (O_I)
32230±40	32200±20	32200±20	$(O—O)_A + 440$: (O_{II})
	32470±30	32470±30	$(O—O)_A + 700$
32700±50	32670±20	32670±20	$(O—O)_A + 910$: (O_{III})
	32900±20	32900±20	$O_{II} + 700$
33250±50	33200±20	33190±20	$O_{II} + 990$
	33350±20	33350±20	$O_{III} + 700$
	33600±40	33600±40	$O_{II} + 1390$
	33670±30	33700±30	$O_{III} + 990$
	33900±50	33900±50	$O_{II} + 700 + 990$
		34100±50	$O_{III} + 1390$
	34180±40	34180±40	$O_{II} + (990 \times 2)$
	34350±40	34350±40	$O_{III} + 700 + 990$
	34680±40	34670±40	$O_{III} + (990 \times 2)$
34950±100	34720±50	34540±50	$(O—O)_B B_{1u} \leftarrow A_{1g}$
	34770±30	34770±30	$O_{III} + 700 + 1390$
34900±40	34870±40	34870±40	$O_{II} + 700 + (990 \times 2)$
	34950±30	34950±30	$O_{II} + (1390 \times 2)$
35100±40	35070±40	35050±40	$O_{III} + 990 + 1390$
35450±50	35220±50	35050±70	$(O—O)_B + 500$
	35160±50	35150±30	$O_{II} + (990 \times 3)$
	35290±30	35290±30	$O_{II} + 700 + 990 + 1390$
35460±50	35450±50	35450±50	$O_{III} + (1390 \times 2)$
36000±100	35800±100	35590±70	$(O—O)_B + 990$
	35650±40	35650±40	$O_{III} + (990 \times 3)$
	35800±40	35800±40	$O_{III} + 700 + 990 + 1390$
	35920±30	35920±30	$O_{II} + 700 + (990 \times 3)$
36450±100	36120±50	35970±50	$(O—O)_B + 1390$
	36160±30	36140±30	$O_{III} + 700 + (1390 \times 2)$
37000±100	36650±50	36450±50	$(O—O)_B + (990 \times 2)$
	36670±30		$O_{III} + (990 \times 4)$
	37090±40		$O_{III} + (990 \times 3) + 1390$
	37250±100	37000±50	$(O—O)_B + 500 + (990 \times 2)$
	37320±40	37310±40	$O_{II} + 990 + (1390 \times 3)$
37800±100	37600±50	37400±50	$(O—O)_B + (1390 \times 2)$
	37700±50		$(O—O)_B + (990 \times 3)$
	38070±40		$O_{III} + (990 \times 4) + 1390$
38300±100	38100±100	37900±70	$(O—O)_B + (990 \times 2) + 1390$
	38350±50		$O_{II} + (990 \times 2) + (1390 \times 3)$
38900±100	38700±100	38550±70	$(O—O)_B + (990 \times 4)$
	39140		$(O—O)_B + (990 \times 3) + 1390$
		39480±70	$(O—O)_B + (990 \times 5)$

TABLE 2 Vibrational Frequencies (cm^{-1}) and Suggested Assignments from the Absorption Spectra in the Vapor and in Doped Rare Gas Solids

1st transition		2nd transition	3rd and 4th transition	Assigned ground state
Vapor[a]	Krypton	Krypton	Krypton	fundamental[b]
437.7	440±30			509 b_{3g}
500.7		500±50		514 a_{1g}
702.0	700±30	700±50	700±100	765 a_{1g}
911.0	910±30			953 b_{3g}
987.4	990±30	990±50	990±100	1021 a_{1g}
1389.5				1380 a_{1g}
	1390±30	1390±50	1390±100	
1434.7				1465 a_{1g}

(a) From Ref. 1: (b) From Ref. 28.

Series II: Progressions in totally symmetric vibrations built upon the " false origin " O—$O_{B_{2u}}$ + 438 cm^{-1} (b_{3g}).

Series III: Progressions in totally symmetric vibrations built upon the false origin O—$O_{B_{2u}}$ + 911 cm^{-1} (b_{3g}).

Series II and III make the major contribution to the total oscillator strength ($f \sim 0.002$)[1] of this transition. There is strong evidence that these series borrow intensity[18,19,30] from the second excited state (oscillator strength of transition ~ 0.1[24]) by the mixing of vibronic states with the same symmetry (B_{1u}) but different electronic parentage.[31]

3.1.1. *Line Widths*

For the naphthalene–rare gas matrices, the line widths of the bands of the first transition (100 cm^{-1}, Kr; 200 cm^{-1}, Xe; 300 cm^{-1}, Ar) are much greater than in the vapor spectrum (1 cm^{-1}). In the latter the line widths are of the order predicted[32] for rotational and sequential broadening. Contributions to the line broadening in the matrix could come from the (1) rapid electronic relaxation induced by the matrix; (2) coupling of states with the lattice vibrations of the host; (3) non-uniformity of the site environment.

The contribution from (1) is expected to be negligible. Although the rate of intersystem crossing from the first excited singlet state of naphthalene increases when the molecule is substituted in rare gas

matrices,[33] this should not lead to appreciable lifetime broadening of the singlet B_{2u} state. The radiative and non-radiative lifetimes are still of comparable order in the matrix ($Q_F/Q_P \sim 0.05$ (Ar)).

Coupling of the excited state with lattice vibrations of the host leads to broadening of the order of kT[33]. This cannot explain the magnitude of the line broadening observed, although the shading to the blue of the absorption bands in the krypton spectrum could result in part from this effect.

Non-uniform site environment appears to be the major source of line broadening. It is interesting to compare the band structure discussed here with that observed in the spectrum of the first π^*–π (singlet) transition of benzene in the same matrices.[34,35] As in the first naphthalene transition, the line broadening due to non-radiative electronic relaxation is negligible. Each member of the principal progression ($O—O(B_{2u} \leftarrow A_{1g}) + e_{2g} + n \times a_{1g}$) is a doublet with a splitting of 70–100 cm^{-1} in the different matrices. It is generally agreed that this splitting arises from the occupation by benzene molecules of inequivalent substitutional sites.[34,35] The line widths (at half intensity) of the doublet components are—15 cm^{-1}, Argon; 30 cm^{-1}, Krypton[34]; and 130 cm^{-1}, Xenon.[36] In benzene doped argon and krypton solids the two major impurity sites seem well defined, although the line widths are still an order of magnitude greater than the corresponding " Shpolskii " lines[37] in a cyclohexane solid solution.[38]

X-ray and electron diffraction data on vapor deposited argon and krypton films[39,40,41,42] show that the metastable hcp phase as well as the usual fcc phase can be formed at low deposition temperatures (below 40 °K) and that impurity molecules can stabilize the hcp phase. Considering the well defined nature of the benzene impurity sites it is probable that they are substitutional sites, possibly in fcc and hcp phases. The line broadening in the naphthalene–rare gas matrix spectra suggests that the molecule may not occupy well defined substitutional sites in the rare gas lattices. A comparison of the " effective size " of the naphthalene molecule (7 Å × 5 Å × 2 Å) with " nearest neighbour " distances for substitutional sites in fcc rare gas lattices (3.75 Å, Ar; 3.99 Å, Kr; 4.33 Å, Xe)[43] seems to support this suggestion. It was noted that line widths in an argon matrix decrease to 100 cm^{-1} at 55 °K (just prior to the host " boiling

off "). This observation is consistent with line broadening arising from a varying site environment. Unfortunately films could not be annealed at 55 °K because of technical difficulties.

The line widths of the absorption bands of the naphthalene–rare gas matrices broaden in the region of the second transition (800 cm^{-1}, Ar (20 °K); 600 cm^{-1}, Ar (55 °K); 600 cm^{-1}, Kr, Xe (20 °K). We associate part of these line widths (1–200 cm^{-1}) with the environmental effect discussed for the first transition. However, a major contribution to the line widths of the bands of the second transition is the lifetime broadening due to the radiationless electronic relaxation of the excited state.[44,45,46] We estimate that in Kr and Xe matrices at 20 °K the radiationless relaxation time is about 10^{-13} sec.

3.1.2. *Vibronic Analysis*

The vapor absorption spectrum is highly congested in the region of the second transition and Sponer and Cooper[2] were unable to assign many of these bands. In the spectra of naphthalene doped argon, krypton and xenon solids (Fig. 1) some narrower bands are superimposed on the broader vibronic bands of the second transition. These bands correspond to progressions in a_{1g} fundamentals built upon the false origins of the first transition (i.e. series II and III). (See Table 1.)

The spectra also reveal that the intensity enhancement of these bands depends strongly on the host and hence the separation between the first and second excited states. For example the overall intensity enhancement is smallest in the argon matrix (see Curve *a*) where the separation between the first and second excited states is greatest. In addition, the intensity patterns vary as the host solid is altered from argon (separation of states 2720 ± 140 cm^{-1}) to krypton (separation of states 2520 ± 70 cm^{-1}) or xenon (separation of states 2340 ± 70 cm^{-1}). The most intense (narrow) band in the argon spectrum (Curve *a*) is at $O_{III}(B_{2u} + 910) + 990 + 1390$ cm^{-1} (shown by a vertical broken line). However in the krypton (Curve *b*) and xenon spectra (Curve *c*) this band is weak compared with the neighbouring members of series II and III, (e.g. $O_{III} + 700 + 1390$ cm^{-1}, $O_{II}(O—O_{B_{2u}} + 440) + 700 + 990 + 1390$ cm^{-1}, see vertical broken lines in Fig. 1B). Unless this effect is due to differences in the geometry of the excited state in the different matrices, it is reasonable

to assume that the intensity patterns are determined by the separation between excited vibronic states of series II and III ($O_{II,III} + n \times a_{1g}$) and the B_{1u} states with which they interact. The position of the $B_{1u} \leftarrow A_{1g}$ electronic origin and vibronic levels are shown by vertical unbroken lines in Fig. 1B. If the enhanced intensity between 280 and 290 nm in individual members of series II and III is due mainly to interaction with the B_{1u} electronic state, the greater relative enhancement of the O_{III} + (990 + 1390) cm^{-1} band in the argon spectrum may be explained by the smaller separation between the excited vibronic state and the B_{1u} electronic state. The separation between the B_{1u} state and the vibronic state giving rise to the band O_{III} + 990 + 1390 cm^{-1} is 150 cm^{-1} argon, 350 cm^{-1} krypton, 510 cm^{-1} xenon. The greater intensity enhancement in some members of series II and III in the krypton spectrum compared with the xenon spectrum (e.g. O_{III} + 700 + 1390 cm^{-1}, O_{III} + 990 + 1390 cm^{-1}) may also be explained by the smaller separation between the excited states of series II and III and the B_{1u} electronic or vibronic states with which they interact (e.g. separation between the bands O_{III} + 700 + 1390 cm^{-1} and (O—O)$B_{1u} \leftarrow A_{1g}$: 50 ± 80 cm^{-1} krypton; 230 ± 80 cm^{-1} xenon). In the krypton spectrum near degeneracy between many members of series II and III and vibronic levels of the second excited state more than offsets the larger separation between the first and second excited states when comparing enhancement effects in krypton and xenon host solids (see Fig. 1B).

The most prominent progressions in series II and III involve the totally symmetric frequencies of 990 cm^{-1} (" breathing ", 1021 cm^{-1} ground state[28]) and 1390 cm^{-1} (central C–C stretch, 1380 cm^{-1} ground state[28]). The longest progressions identified involve four quanta of the 990 cm^{-1} vibration and three quanta of the 1390 cm^{-1} vibration (see Table 1). Because of varying intensity enhancement in members of these progressions it is not possible to deduce anything meaningful about the Franck-Condon envelope.

In the second transition the most prominent progressions again involve the 990 cm^{-1} and 1390 cm^{-1} frequencies, the longest progression involving four quanta of the 990 cm^{-1} frequency. The most intense band in this transition is at $(O—O)_{B_{1u}}$ + (1 × 1390) cm^{-1} (see Table 1).

In the absorption spectra of naphthalene vapor[1] and naphthalene

doped durene[7] the longest progressions identified in the first transition involve two quantum intervals in the 990 cm^{-1} and 1390 cm^{-1} frequencies. The conclusions were[1,7] that the molecular geometry changed little upon excitation, the only appreciable change probably involving a slight increase in ring size and a lengthening of the central C—C link. The identification of longer progressions in the 990 cm^{-1} and 1390 cm^{-1} frequencies in the naphthalene–rare gas matrix spectra might indicate larger changes in the excited state geometry of the molecule in such matrices than in the isolated molecule. But the intensity enhancement and redistribution which arise in the rare gas matrices because of the smaller separation of the excited states makes any definite conclusion difficult.

3.2. Spectral Region 250 nm–125 nm

Figure 2 shows the absorption spectrum of a naphthalene–krypton matrix (molar ratio 1 : 200) between 125 and 250 nm (40000 to 80000 cm^{-1}). Transition energies and assignments are given in Table 3.

The free molecule spectrum above 40000 cm^{-1} exhibits extra valence (Rydberg) transitions.[25] There is a higher density of electronic states (both π^* and Rydberg) carrying oscillator strength from the ground state and the density of background vibronic levels provided by the lower π^* states approaches that of a " quasi continuum ".[44,45] Rapid radiationless decay into this quasi continuum leads to extensive level broadening in these higher electronic states. One also sees features due to configuration interaction between the Rydberg states and the quasi continuum of the inhomogeneously broadened π^*–π states.[27]

In the matrix one expects the Rydberg states of the guest molecule to be strongly perturbed by the host.[47,48,49] Even in the gas at high pressures of an inert perturbing gas (100 atms of N_2 or He) the Rydberg bands become asymmetrically broadened.[50] In the condensed state, the medium would severely perturb the overlapping Rydberg orbital and the impurity state can no longer be treated adequately within a " Frenkel " tight binding description.

3.2.1. *Large Radius Impurity States of the Matrix*

The assignment of absorption bands around 55000 cm^{-1} to

TABLE 3 Transition Energies (cm^{-1}) and Suggested Assignments in the Absorption Spectra of Naphthalene in Doped Rare Gas Solids (250 nm–125 nm)

Matrix isolation spectrum			
Argon	Krypton	Xenon	Suggested assignments
46100±50	45500±50	44900±50	$(O—O)_A B_{2u} \leftarrow A_{1g}(\pi^*-\pi)$
46800±50	46250±50	45650±50	$(O—O)_A + 700$
	46500±50		$(O—O)_A + 990$
47450±50	46900±50	46300±50	$(O—O)_A + 1390$
48300±100	47600±50	47100±100	$(O—O)_B B_{1u} \leftarrow A_{1g}(\pi^*-\pi)$
	47850±50		$(O—O)_A + 990 + 1390$
48900	48700±50	48400±100	$(O—O)_{C/D}$ $R^3 \leftarrow N$?
49550	49400±50	49100±100	$(O—O)_{C/D} + 700$ $(R^3 \leftarrow N) + 700$?
	50500±100		$(O—O)_B + 1390 \times 2$; $(O—O)_B + 990 \times 3$
	51150±100		$(O—O)_B + 700 + (1390 \times 2)$?
52740±100	54600±100	53800±100	$n = 2$ Wannier impurity state
55400±100	56500±100	54900±100	$n = 3$ Wannier impurity state
58000±200	57800±100	56800±100	$(O—O)_E B_{2u} \leftarrow A_{1g}$? $(\pi^*-\pi)$?
	58500±100		$(O—O)_E + 700$
62000±200	61200±200	61200±200	$B_{1u} \leftarrow A_{1g}$? $(\pi^*-\pi)$?
68500±500	67100±200	Absorption	?
	75000±200	by host	?

$n = 2$ and $n = 3$ Wannier impurity states has been discussed elsewhere.[51] In most solids, such large radius states are not amenable to experimental observation because of the rapid electronic relaxation (and accompanying line broadening) which arises from efficient scattering of the excited electron by the medium. However as predicted by Rice and Jortner,[52] the electron mobility in rare gas solids is such that large radius excited states are observable[53] with line widths of the order of 100 cm^{-1}.

In these doped solids, the binding energies of large radius impurity states are small compared with the band gap and the Wannier weak coupling model is applicable. The predicted impurity energy levels assuming the impurity potential can be replaced by a hydrogenic potential in a uniform dielectric are given by

$$E_n = I_s - G/n^2$$

where I_s is the ionization potential of the impurity in the solid and $G = Rm^*/X^2$ (R is the Rydberg constant, m^* is an appropriate effective mass, X is the static dielectric constant of the solid).

I_s is related to the threshold energy for photoemission (F) in the solid by the expression

$$I_s = F + V_0 = (I_g + P_+) + V_0$$

where I_g is the ionization potential of the isolated guest molecule, P_+ is the polarization energy of the host solid by the positive impurity hole, V_0 is the energy of the quasi-free excess electron in the medium. We have previously reported the value of F in these matrices.[51] Treating the photoemission yield curves by the recent analytic method of Marchetti and Kearns[54] a more reliable value of the threshold energy F is obtained. In Table 4 we summarize the observed photoemission thresholds and energies of Wannier impurity states and the deduced crystal energy parameters. Such parameters compare favourably with the values calculated from spectroscopic[55] and photoelectric[56] studies of benzene–rare gas matrices and spectroscopic studies of pure rare gas solids.[57,58,59]

To check our experimental value of F, which might have been affected by surface impurities and crystalline disorder possible in low temperature vapor deposited films, we have performed photoemission experiments on naphthalene films. These films were

TABLE 4 Observed Photoemission Thresholds and Energies (in eV) of Wannier States with Deduced Crystal Energy Parameters for Naphthalene–Rare Gas Solids

	Argon matrix (20 °K)	Krypton matrix (20 °K)	Xenon matrix (20 °K)
$n = 2$	6.54 ± 0.01	6.77 ± 0.01	6.67 ± 0.01
$n = 3$	6.87 ± 0.01	7.01 ± 0.01	6.81 ± 0.01
I_s	7.14 ± 0.05	7.20 ± 0.05	6.93 ± 0.05
G	2.40 ± 0.04	1.72 ± 0.04	1.04 ± 0.04
F	7.45 ± 0.10	7.45 ± 0.10	7.28 ± 0.10
P^+	-0.69 ± 0.10	-0.69 ± 0.10	-0.86 ± 0.10
V_0	-0.31 ± 0.15	-0.25 ± 0.15	-0.35 ± 0.15

deposited under identical conditions (40 °K) and the threshold for electron photoemission determined. The value of F determined using a similar analytic method is 6.7 • 0.1 eV which may be compared to the single crystal value 6.8 eV reported by Lyons and Morris.[60]† We deduce that surface contamination should not be affecting our values of F for naphthalene–rare gas solids.

Finally we note that the lines we assign to the $n = 2$ and $n = 3$ Wannier impurity states might conceivably be related to the lowest free molecule Rydberg transitions identified[26] in the vapor spectrum at 45070 cm^{-1} and 45390 cm^{-1}. However, the medium shifts do not increase systematically, Xe < Kr < Ar and the blue shifts necessary to support this explanation (0.3–0.6 eV) are much smaller than observed (0.95 eV, Ar; 1.2 eV, Kr; 1.1 eV, Xe).

3.2.2. *Intermediate Radius Impurity States of the Matrix*

When the radius of the excited impurity state is comparable with the lattice spacing, overlap of the excited electron with the medium is still too large to justify use of a simple tight binding description. On the other hand the radius of the excited state is not large enough to justify the simple effective mass approximation. In this case the description chosen is often a matter of convenience. A modified tight binding description may be used which allows for non-orthogonality effects[61,62,63] and for charge delocalization.[64] Alternatively, a Wannier description may be used and central cell

† We note that the photemission threshold for a single crystal differs little from that of a polycrystalline film.

corrections introduced.[65,66] Impurity states arising from the lowest Rydberg state of an impurity molecule in a rare gas solid fall within the above category. Modified tight binding descriptions[63,64] predict medium blue shifts of 0–1 eV for transitions to the lowest Rydberg states of small atoms in rare gas solids. These predictions agree well with the blue shifts 0.3–0.6 eV reported for the lowest Rydberg transitions of small atoms and molecules in these solids.[47,49,67]

The lowest free molecule Rydberg transitions of naphthalene have been reported[26] at 45090 cm^{-1} and 45390 cm^{-1}. In the spectrum of a naphthalene–kepton matrix (see Fig. 2) two lines are observed in

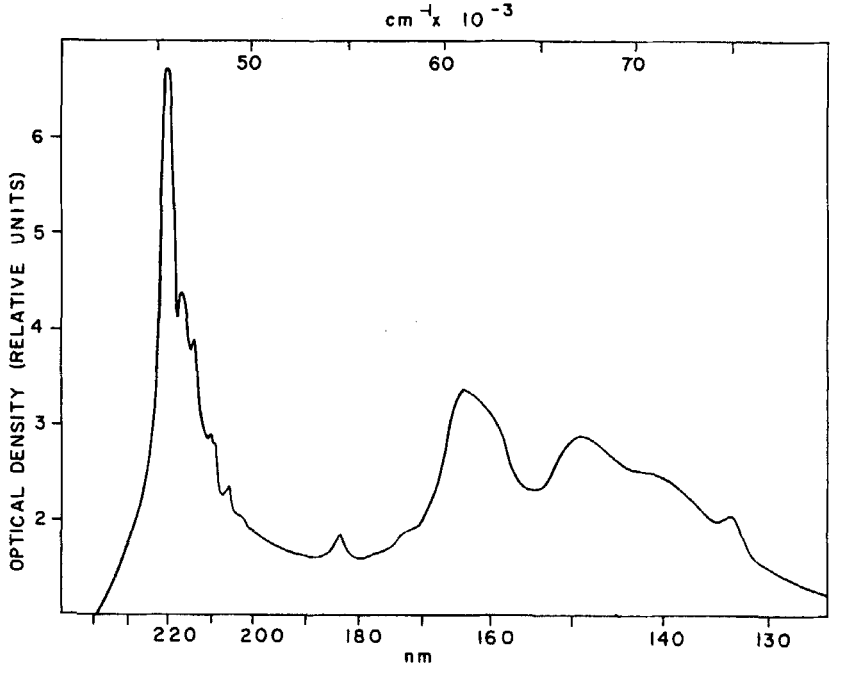

Figure 2. The absorption spectrum from 250 nm to 125 nm of naphthalene doped krypton solid at 20 °K. Deposition temperature 40 ± 2 °K, molar ratio (naphthalene–krypton) 1 : 200.

the region of 204 nm (48000–49000 cm^{-1}) which do not appear to have counterparts in the π^*–π absorption spectrum of the vapor and cannot be assigned as vibrational bands of the third and fourth π^*–π transitions (see Table 3). The lower energy line has been assigned to the free molecule Rydberg transition $R_b^3 \leftarrow N$ and

$R_c^3 \leftarrow N$ (not resolved in the matrix spectrum because of line broadening) from the following evidence.

(i) *Isotope Shifts.* This line shifts 20 ± 100 cm^{-1} to the blue on complete deuteration of the molecule (*cf.* isotope shifts in Rydberg transitions of the free molecule).

(ii) *Medium Shifts.* The calculated medium shifts $(\bar{\nu}_{solid} - \bar{\nu}_{vapo})_r$ of this line and corresponding lines in Ar and Xe matrices are: 3780 ± 80 cm^{-1} (Ar); 3630 ± 80 cm^{-1} (Kr); 3350 ± 80 cm^{-1} (Xe). These blue shifts are similar to those reported for the lowest Rydberg transitions of small molecules in rare gas matrices. However it is noted that dependences of the medium shift on the host are not as marked as those reported by Katz *et al.* for benzene doped matrices.[55]

(iii) *Vibronic Analysis.* The spacing between the two bands is 700 ± 100 cm^{-1} in all matrices. In the naphthalene vapor spectrum[26] one of the vibronic bands assigned to the lowest Rydberg transitions was at $(O—O)_{RB}3 + 750 \pm 50$ cm^{-1}. Failure to identify further vibronic bands in the matrix spectrum may be due to line broadening and spectral congestion.

3.2.3. π^* *States* (250 nm–200 nm)

Two π^*–π transitions are predicted in this region 47 900 cm^{-1} ($f = 2.1$; $B_{2u} \leftarrow A_{1g}$) and 50 900 cm^{-1} ($f = 0.7$; $B_{1u} \leftarrow A_{1g}$) from a Pariser-Parr semi-empirical treatment with limited configuration interaction.[19] However Allinger and Stuart,[21] using a self-consistent field modification of the Pariser-Parr treatment and invoking extensive configuration interaction predict these two transitions to be quasi degenerate (see Table 5). The origin of the third transition has been reported in the vapor spectrum at 47 500 cm^{-1} ($f \approx 1.0$) and a shoulder at 49 500 cm^{-1} ($f \approx 0.3$) tentatively assigned to the fourth transition.[24] These assignments are confirmed in the present work by: (i) analysis of the vibronic structure which is better resolved in the matrix spectrum; (ii) measurement of the matrix shifts of different bands; (iii) measurement of deuterium isotope shifts.

(i) *Vibronic Structure.* The vibronic structure is best resolved in the krypton matrix spectra. There is still, of course, line broadening due to rapid intramolecular relaxation but the invariance of the line

TABLE 5 The Experimental and Predicted Transition Energies of the $\pi^*-\pi$ Transitions of Naphthalene.

Pariser[19]	Hummel and Ruedenberg[20]	Allinger and Stuart[21]	Experimental
32400 ($f\sim0.0$)	33700 ($f\sim0.03$)	33500	32020[a] ($f\sim0.02$)
36200 ($f\sim0.26$)	36500 ($f\sim0.21$)	39000	35910[b] ($f\sim0.1$)[c]
47900 ($f\sim2.1$)	48900 ($f\sim2.4$)	52300	47370[d] ($f\sim1.0$)
51000 ($f\sim0.7$)	49200 ($f\sim0.7$)	52300	49400[d] ($f\sim0.3$)
64200 ($f\sim0.04$)	62000 ($f\sim0.1$)		57800[e] ($f\sim0.1$)
66000 ($f\sim1.01$)	66500 ($f\sim1.01$)		61200[e] ($f\sim1$)

(a) Vapor value, Ref. 1; (b) Vapor value, Ref. 2; (c) Vapor value, Ref. 24; (d) Vapor value, this work; (e) Value in krypton matrix 20 °K.

widths from vapor to matrix (600 cm^{-1}) indicates that "matrix broadening" is not important in these higher transitions. The transition energies and assignments have been given in Table 3. All absorption features above 45000 cm^{-1} in the matrix spectra (excluding the intermediate and large radius impurity states discussed earlier) may be related to origin bands at 45500 cm^{-1} and 47600 cm^{-1} (in a krypton matrix) and vibronic bands (700, 990 and 1390 cm^{-1}) built on these origins. The vibrational intervals are summarized in Table 2.

(ii) *Matrix Shifts.* The matrix shifts ($\bar{\nu}_{\text{matrix}} - \bar{\nu}_{\text{vapor}}$) of the origin bands are given in Table 6. The origin bands for the first three transitions both in the vapor and solid are readily located but there is difficulty in locating the electronic origin accurately for the fourth transition in the vapor. The consistency of the matrix shift with the transition energy (49400 cm^{-1}) and oscillator strength ($f\sim0.3$) of the transition may be checked using Longuet-Higgins and Pople's formulation.[68] They express the dispersive red shift ($\Delta\bar{\nu}$) of the electronic transition of a non-polar molecule in a non-polar solvent as

$$\Delta\bar{\nu} = -\tfrac{1}{6}\alpha_B Z\bar{R}^{-6}[\tfrac{1}{4}E_i\alpha_A + M^2_{0\to i}]$$

where α_B is the average electric polarizability of the solvent molecule.

Z is the effective number of nearest neighbour solvent molecules.

$\bar{R}$ is the mean solute-solvent separation.

TABLE 6 Medium Shifts of Transition Energies (cm^{-1}) of Naphthalene Molecule in Rare Gas Solids

Matrix	First transit[a]	Second transit[b]	Third transit	Fourth transit
	$B_{2u}\leftarrow A_{1g}$ ($f\sim0.002$)	$B_{1u}\leftarrow A_{1g}$ ($f\sim0.14$)	$B_{2u}\leftarrow A_{1g}$ ($f\sim1$)	$B_{1u}\leftarrow A_{1g}$ ($f\sim0.3$)
Argon	220 ± 50	960 ± 100	1300 ± 100	1100 ± 100
Krypton	250 ± 20	1190 ± 50	1900 ± 100	1800 ± 100
Xenon	270 ± 20	1370 ± 50	2500 ± 100	2300 ± 100

(a) $\bar{\nu}_{vap}$ taken from Ref. 1; (b) $\bar{\nu}_{vap}$ taken from Ref. 2.

E_i is the transition energy of the solute.

α_A is the average electric polarizability of the solute molecule.

$M_{0\to i}$ is the transition dipole moment for the solute transition.

The expression assumes (a) there is a random angular distribution of isotropic solvent molecules about the isotropic guest; (b) the average polarizability of the solute (α_A) is the same in the ground and excited states; (c) $E_i \ll \bar{E}$ (the average excitation energy of the solute) $\approx \bar{F}$ (the average excitation energy of the solvent).

These assumptions are not valid for the higher π^*–π transitions of naphthalene in rare gas solids and Eq. (1) is expected to be very approximate. As Z and $\bar{R}$ are not known and the guest molecule is highly anisotropic, only the ratio of the shifts was calculated for transitions of the same polarization in the same host. The ratio of the matrix shifts for the second and fourth transitions (both assumed to be short axis polarized ($B_{1u} \leftarrow A_{1g}$) was predicted from the following data.

$$\alpha_A = 175 \times 10^{-25}\ \text{cm}^{-3}\ [69]$$
$$E_2 = 36000\ \text{cm}^{-1}[12];\ f_2 = 0.14[24]$$
$$E_4 = 49500\ \text{cm}^{-1};\ f_4 = 0.3[24]$$

The predicted shift ratio ($\Delta\bar{\nu}_4 : \Delta\bar{\nu}_2$) is 1.41 : 1 while the measured ratios are 1.7 ± 0.2 ; 1 (Xenon); 1.5 ± 0.2 : 1 (Krypton); 1.1 ± 0.2 : 1 (Argon). Considering the approximations made the agreement appears reasonable.

(iii) *Deuterium Isotope Shifts.* The electronic origins of the first and second π^*–π transitions shift 118 cm^{-1} and 130 cm^{-1} respectively to the blue on complete deuteration.[1,2] The deuterium isotope shifts of the bands at 47370 and 49380 cm^{-1} in the vapor spectrum are 130 ± 100 cm^{-1} and 200 ± 100 cm^{-1} respectively.

3.2.4. π^* *States* (200 nm–125 nm)

The absorption spectrum of a naphthalene–krypton matrix between 125 nm and 250 nm is included in Fig. 2. The spectral features are:

(i) Two bands near 55000 cm^{-1} (line widths ~500 cm^{-1}) which have been previously discussed as transitions to Wannier impurity states of the solid.

(ii) Two shoulders (separated by $\sim$700 cm^{-1}) near 58000 cm^{-1} which we suggest arise from a π^*–π transition.

The bands shift 130 $\pm$ 100 cm^{-1} to the blue on complete deuteration which supports this suggestion. Further, the vibration interval of 700 cm^{-1} between these shoulders is identical to that between the origin band of the third π^*–π transition and the most intense vibronic band built on this origin. Hence, we assign the band 58000 cm^{-1} to a π^*–π transition and the band 58700 cm^{-1} as a vibronic band built on this. It is not possible to measure a matrix shift because this π^*–π transition is obscured by the intense Rydberg bands in the vapor spectrum.

(iii) Three broad bands near 61000, 67000 and 75000 cm^{-1}, the lowest and most intense of which probably marks the π^*–π transition seen near 62000 cm^{-1} in the vapor. The matrix shift of this band increases as the host matrix is altered from Ar to Kr to Xe.

Above 50000 cm^{-1}, the predicted energies and intensities of π^*–π transitions become unreliable. In Table 5 the predicted energies of the higher π^* states are compared with the positions of the absorption peaks identified in the matrix spectrum. The shoulder in the Kr matrix spectrum at 57800 cm^{-1} is assigned to the $B_{2u} \leftarrow A_{1g}$ transition predicted near 63000 cm^{-1}. The strong absorption maximum at 61000 cm^{-1} is assigned to the $B_{1u} \leftarrow A_{1g}$ transition predicted near 66000 cm^{-1}.

For the bands near 67000 cm^{-1} and 75000 cm^{-1} an assignment to π^* states is difficult. Bond dissociation processes and other open photochemical channels as well as transitions to states of the positive ion must contribute to the intensity in this region. In the absence of adequate data on such processes it seems unrealistic to assign the spectral features above 65000 cm^{-1} to any specific transitions.

Acknowledgements

We thank the Australian Research Grants Committee for financial support.

REFERENCES

1. Craig, D. P., Hollas, J. M., Redies, M. F. and Wait, S. C., *Phil. Trans. Faraday Soc.* **A253,** 543 (1961).

2. Sponer, H. and Cooper, C. D., *J. Chem. Phys.* **23**, 646 (1955).
3. Hollas, J. M., *J. Mol. Spect.* **9**, 138 (1962).
4. Ferguson, J., Reeves, L. W. and Schneider, W. G., *Can. J. Chem.* **35**, 1117 (1959).
5. Koyanagi, M., *J. Mol. Spect.* **25**, 273 (1968).
6. Zimmerman, H. and Yoop, N., *Z. Elektrochem.* **64**, 1219 (1960).
7. McClure, D. S., *J. Chem. Phys.* **22**, 1668 (1954); **24**, 1 (1956).
8. Bolotnikova, T. N., *Izv. Akad. Nauk. SSSR. Ser. Fiz.* **23**, 28 (1959).
9. Bree, A. and Thirunamachandran, T., *Mol. Phys.* **5**, 397 (1962).
10. Prikhot'ko, A. F. and Soskin, M. S., *Opt. Spect.* **13**, 291 (1962).
11. Broude, V. L., *Opt. Spect.*, Suppl. **2**, 25 (1967).
12. Colson, S. D., Hanson, D. M., Kopelman, R. and Robinson, G. W., *J. Chem. Phys.* **48**, 2215 (1968).
13. See for example—Löwdin, P. O. and Pullman, B. (Ed.), " Molecular Orbitals in Chemistry Physics and Biology" (Academic Press, 1964).
14. See for example—Murrel, J. N., " The Theory of the Electronic Spectra of Aromatic Molecules" (Methuen, 1963).
15. Davydov, A. S., " The Theory of Molecular Excitons" (McGraw-Hill, 1962).
16. Knox, R. S., " Theory of Excitons" (Academic Press, 1963).
17. Rice, S. A. and Jortner, J., " Physics and Chemistry of the Organic Solid State" (Ed. Labes, M. M. and Weissberger, A.; Interscience) **3**, 201 (1967).
18. Herzberg, G., " Electronic Spectra and Electronic Structure of Polyatomic Molecules" (Van Nostrand, D., 1967), p. 141.
19. Pariser, R., *J. Chem. Phys.* **24**, 250 (1956).
20. Hummel, R. L. and Ruedenberg, K., *J. Phys. Chem.* **66**, 2335 (1962).
21. Allinger, N. L. and Stuart, T. M., *J. Chem. Phys.* **47**, 4611 (1967).
22. Skanke, P. N., *Acta. Chem. Scand.* **18**, 1671 (1964).
23. Klevens, H. B. and Platt, J. R., *J. Chem. Phys.* **17**, 470 (1949).
24. George, G. A. and Morris, G. C., *J. Mol. Spect.* **26**, 67 (1968).
25. Angus, J. G., Christ, B. J. and Morris, G. C., *Aust. J. Chem.* **21**, 2153 (1968).
26. Angus, J. G. and Morris, G. C., *Aust. J. Chem.* (to be published).
27. Jortner, J. and Morris, G. C., *J. Chem. Phys.* **51**, 3689 (1969).
28. Suzuki, M., Tokoyama, Y, and Ito, M., *Spectrochim. Aita.* **24A**, 1091 (1968).
29. Herzberg, G. and Teller, E., *Z. Physik. Chem.* **B21**, 410 (1933).
30. Albrecht, A. C., *J. Chem. Phys.* **33**, 169 (1960).
31. Jortner, J., Rice, S. A. and Hochstrasser, R. M., " Advances in Photochemistry " (Ed. Pitts, J. N., Hammond, G. S., Noyes, W. A.; Interscience) **7**, 175 (1969).
32. Byrne, J. P. and Ross, I. G., *Canad. J. Chem.* **43**, 3253 (1965).
33. Robinson, G. W., *J. Mol. Spect.* **6**, 58 (1961).
34. Diamant, Y., Hexter, R. M. and Schnepp, O., *J. Mol. Spect.* **18**, 158 (1965).
35. Hollier, E. W. and Blount, C. E., *J. Mol. Spect.* **19**, 456 (1966).
36. Angus, J. G. and Morris, G. C.—Unpublished results.
37. Taylor, A. H., *Chem. Phys. Letters* **5**, 111 (1970).
38. Leach, S. and Lopez-Delgado, R., *J. Phys.* **28** (Suppl.) C3-150 (1967).
39. Barrett, C. S., Haasen, P. and Meyer, L., *J. Chem. Phys.* **40**, 2744 (1964).
40. Barrett, C. S. and Meyer, L., *J. Chem. Phys.* **41**, 1078 (1964).

41. Curzon, A. E. and Pawlowicz, A. I., *Proc. Phys. Soc.* (*Lond.*) **85**, 375 (1965).
42. Kovalenko, S. I. and Bagrov, N. N., *Fiz. Tverd. Tela.* **9**, 3032 (1967).
43. Roncin, J. Y., *Chem. Phys. Letters* **3**, 408 (1969).
44. Robinson, G. W., *J. Chem. Phys.* **47**, 1967 (1967).
45. Bixon, M. and Jortner, J., *J. Chem. Phys.* **48**, 715 (1968).
46. Henry, R. B. and Kasha, M., *Am. Rev. Phys. Chem.* **19**, 161 (1968).
47. McCarty, M. and Robinson, G. W. *Mol. Phys.* **2**, 415 (1959).
48. Roncin, J. Y., Damany, N. and Romand, J., *J. Mol. Spect.* **22**, 154 (1967).
49. Katz, B. and Jortner, J., *Chem. Phys. Letters* **3**, 437 (1968).
50. Robin, M. B. and Kuebler, N. A., *J. Mol. Spect.* **33**, 274 (1970).
51. Angus, J. G. and Morris, G. C., *Chem. Phys. Letters* **5**, 480 (1970).
52. Rice, S. A. and Jortner, J., *J. Chem. Phys.* **44**, 4470 (1967).
53. Miller, L. S., Howe, S. and Spear, W. E., *Phys. Rev.* **166**, 871 (1968).
54. Marchetti, A. D. and Kearns, D. R., *Mol. Cryst. and Liq. Cryst.* **6**, 299 (1970).
55. Katz, B., Brith, N., Sharf, B. and Jortner, J., *J. Chem. Phys.* **50**, 5195 (1969).
56. Angus, J. G. and Morris, G. C., *Mol. Cryst. and Liq. Cryst.* (in press).
57. Steinberger, L. T. and Schnepp, O., *Solid State Comm.* **5**, 417 (1967).
58. Baldini, G., *Phys. Rev.* **128**, 1562 (1962).
59. See Raz, B. and Jortner, J., *Chem. Phys. Letters* **4**, 155 (1969) and the references to the work of R. Haensl *et al.*
60. Lyons, L. E. and Morris, G. C., *J. Chem. Soc.* 5192 (1960).
61. Knox, R. S., *Phys. Rev.* **110**, 375 (1958).
62. Gold, A., *Phys. Rev.* **124**, 1740 (1961).
63. Bhargava, R. K. and Dexter, D. L., *Phys. Rev., B.* **1**, 1 (1970).
64. Weber, S., Rice, S. A. and Jortner, J., *J. Chem. Phys.* **42**, 1907 (1965).
65. Phillips, J. C., *Phys. Rev.* **136**, A1705, A1714 (1964).
66. Hermanson, J., *Phys. Rev.* **150**, 660 (1966).
67. Roncin, J. Y., Damany, D. and Vodar, B., *Chem. Phys. Letters* **3**, 197 (1969).
68. Longuet-Higgins, H. C. and Pople, J. A., *J. Chem. Phys.* **27**, 192 (1957).
69. Amos, A. T. and Hall, G. C., *Theoret. Chem. Acta* **6**, 146 (1964).